

Probing the anomalous triple $ZZ\gamma$ and $Z\gamma\gamma$ couplings at the FCC- μp and SPPC- μp

Emre Gurkanli^{*1}

¹*Department of Physics, Sinop University, Turkey.*

(Dated: March 18, 2024)

Abstract

In this study, 24.5 TeV CoM energy FCC- μp and 20.2 TeV CoM energy SPPC- μp muon-proton colliders have been utilized to explore the anomalous $ZZ\gamma$ and $Z\gamma\gamma$ couplings corresponding to dim-8 operators through the process of $\mu^-\gamma \rightarrow Zl^- \rightarrow l^-\bar{\nu}_l\nu_l$. A cut-based method has been applied to enhance the signal background ratio in the analysis. Coupling limits, at a 95% Confidence Level (C.L.), under the systematic uncertainties of 0%, 3%, and 5%, were obtained with luminosities of $\mathcal{L}_{int} = 5$ and 42.8 fb^{-1} for FCC- μp and SPPC- μp colliders, respectively. The limits for anomalous C_{BB}/Λ^4 , $C_{\tilde{B}W}/\Lambda^4$, C_{WW}/Λ^4 , C_{BW}/Λ^4 couplings without systematic uncertainty for FCC- μp and SPPC- μp were found as follows, respectively: [0.06845; 0.070019967] TeV-4, [-0.18662; 0.18422] TeV-4, [-0.23623; 0.23815] TeV-4, [-0.61912; 0.62072] TeV-4, and [-0.06606; 0.05050] TeV-4, [-0.15791; 0.15126] TeV-4, [-0.20663; 0.19155] TeV-4, [-0.51383; 0.52211] TeV-4.

PACS numbers: 12.60.-i, 14.70.Bh, 14.70.Hp

Keywords: Electroweak interaction, Anomalous couplings, Models beyond the Standard Model.

^{*} egurkanli@sinop.edu.tr

I. INTRODUCTION

The Standard Model stands as a successful theory interpreting the behavior of fundamental particles and their interactions within reachable energy constraints at present collider experiments. However, a more comprising theory is required to address unresolved issues in the universe such as the strong CP problem, non-zero neutrino masses and the baryon asymmetry in the early universe. The self-interactions of the gauge bosons are described by the non-Abelian gauge symmetry of the SM. These interactions can be defined by triple gauge boson couplings, WWV, ZZV , and $ZV\gamma$ ($V=\gamma, Z$) [1]. However, interactions involving the photon and Z -boson are not present at the lowest order in the SM, as the Z -boson has no electric charge. The absence of $ZZ\gamma$, $Z\gamma\gamma$, and ZZZ triple interactions in the SM leads to deviations from SM predictions in the presence of these vertices, providing sensitive evidence for new physics. In the literature, aTGC have been extensively investigated in various production processes in ee [2–18] and pp [19–29] colliders. Studies in accelerator physics that contains a variety of collision types play a crucial role in advancing research on new physics within particle physics [30–32]. The LHC is a high-potential Hadron collider designed to explore new particles and interactions. However, the final state jets scattered after the collision of proton beams lead to complex backgrounds, making it challenging to make precise measurements at the LHC to detect the signals. As the most potent and expansive circular proton-proton collider ever constructed, the LHC is set to undergo gradual enhancements through advancing accelerator technology. Pursuing novel physics beyond the Standard Model (SM), lepton-hadron colliders are promising contenders in the trajectory of particle physics. After the LHC era, the strategy entails converting the LHC into the LHeC by adding an electron ring adjacent to the primary LHC tunnel. Subsequent phases involve substituting the electron ring with a muon counterpart, establishing a new lepton-hadron collider named LHC- μp . On the other hand, the FCC is planned to be a circular collider at CERN for the post-LHC epoch. The FCC initiative involves the conceptualization of a forthcoming ee collider, with plans to incorporate pp , ep , $\mu\mu$, and μp colliders. Notably, FCC-hh is envisioned as a future pp collider boasting a CoM energy of 100 TeV [33]. Introducing a muon ring addition to the FCC will facilitate the formation of high energy μp colliders [34]. Simultaneously, a pp collider named Super Proton Proton Collider (SPPC) with a CoM energy of 70 TeV was designed in China. Preceding the SPPC

collider, the CEPC is planned as the initial phase utilizing the same tunnel and is envisaged as the future ee collider. The CEPC/SPPC project includes $\mu\mu$, ep , and μp collisions to be conducted in later years, similar to the FCC project [35]. Many phenomenological studies have been done in muon colliders [36–64]. This study focuses on the FCC- μp and SPPC- μp colliders, which have high CoM energies and high luminosity values. The values used for the FCC- μp collider are $E_\mu = 3$ TeV, $E_p = 50$ TeV, $\mathcal{L}_{int} = 5 \text{ fb}^{-1}$, and for the SPPC- μp collider, $E_\mu = 1.5$ TeV, $E_p = 68$ TeV, $\mathcal{L}_{int} = 42.8 \text{ fb}^{-1}$.

The Effective Field Theory (EFT) is a useful tool to investigate potential new physics phenomena beyond the SM. Exploring aNTGC within the framework of the SM gauge group necessitates the addition of higher order dimension operators into the SM Lagrangian. These operators introduce anomalous couplings, influencing the effective vertices[12]. The focus of this study lies in examining dim-8 operators that characterize aNTGC. Thus, the effective Lagrangian, including SM interactions and new physics contributions, is given by [65].

$$\mathcal{L}^{\text{NTGC}} = \mathcal{L}_{\text{SM}} + \sum_i \frac{C_i}{\Lambda^4} (\mathcal{O}_i + \mathcal{O}_i^\dagger) \quad (1)$$

Here, Λ represents the scale of new physics, while the coefficients C_i denote dimensionless parameters associated with the new physics. The dim-8 operators \mathcal{O}_i are expressed in the following equations.

$$\mathcal{O}_{\tilde{B}W} = iH^\dagger \tilde{B}_{\sigma\lambda} W^{\sigma\mu} \{D_\mu, D^\lambda\} H, \quad (2)$$

$$\mathcal{O}_{BW} = iH^\dagger B_{\sigma\mu} W^{\sigma\rho} \{D_\rho, D^\mu\} H, \quad (3)$$

$$\mathcal{O}_{WW} = iH^\dagger W_{\sigma\mu} W^{\sigma\rho} \{D_\rho, D^\mu\} H, \quad (4)$$

$$\mathcal{O}_{BB} = iH^\dagger B_{\sigma\mu} B^{\sigma\nu} \{D_\nu, D^\mu\} H \quad (5)$$

where

$$B_{\mu\nu} = (\partial_\mu B_\nu - \partial_\nu B_\mu), \quad (6)$$

$$W_{\mu\nu} = \sigma^i (\partial_\mu W_\nu^i - \partial_\nu W_\mu^i + g\epsilon_{ijk}W_\mu^j W_\nu^k), \quad (7)$$

with $\langle \sigma^j \sigma^i \rangle = \delta^{ji}/2$ and

$$D_\mu \equiv \partial_\mu - i\frac{g'}{2}B_\mu Y - ig_W W_\mu^i \sigma^i. \quad (8)$$

In these equations $B_{\mu\nu}$ and $W_{\mu\nu}$ represent the field strength tensors, H is the Higgs field, and D_μ stands for the covariant derivative. On the other hand, $\mathcal{O}_{\tilde{B}W}$ is CP conserving while the \mathcal{O}_{BW} , \mathcal{O}_{WW} and \mathcal{O}_{BB} are CP -violating operators.

In the high energy region, the most significant contribution is the interference between dim-8 operators and the SM. Dim-6 operators have no impact at the tree level on aNTGC, but at one-loop, there is an effect on aNTGC proportional to $\alpha\hat{s}/4\pi\Lambda^2$. In the context of tree-level interactions, the effects of dim-8 operators become at the $v^2\hat{s}/\Lambda^4$ level. These surpass the one-loop effects originating from dim-6 operators when $\Lambda \lesssim \sqrt{4\pi\hat{s}/\alpha}$ [65]. The effective Lagrangian containing dim-6 and dim-8 operators is given in [66].

$$\begin{aligned} \mathcal{L}_{\text{aNTGC}}^{\text{dim-six,eight}} = & \frac{e}{m_Z^2} \left[-[f_4^\gamma(\partial_\alpha F^{\alpha\beta}) + f_4^Z(\partial_\alpha Z^{\alpha\beta})]Z_\mu(\partial^\mu Z_\beta) + [f_5^\gamma(\partial^\beta F_{\beta\mu}) + f_5^Z(\partial^\beta Z_{\beta\nu})]\tilde{Z}^{\nu\alpha}Z_\alpha \right. \\ & - [h_1^\gamma(\partial^\beta F_{\beta\mu}) + h_1^Z(\partial^\alpha Z_{\alpha\mu})]Z_\beta F^{\mu\beta} - [h_3^\gamma(\partial_\beta F^{\beta\rho}) + h_3^Z(\partial_\beta Z^{\beta\lambda})]Z^\sigma\tilde{F}_{\lambda\sigma} \\ & - \left\{ \frac{h_2^\gamma}{m_Z^2}[\partial_\rho\partial_\beta\partial^\alpha F_{\alpha\nu}] + \frac{h_2^Z}{m_Z^2}[\partial_\rho\partial_\beta(\square + m_Z^2)Z_\nu] \right\} Z^\rho F^{\nu\beta} \\ & \left. + \left\{ \frac{h_4^\gamma}{2m_Z^2}[\square\partial^\sigma F^{\rho\alpha}] + \frac{h_4^Z}{2m_Z^2}[(\square + m_Z^2)\partial^\rho Z^{\alpha\beta}] \right\} Z_\rho\tilde{F}_{\alpha\beta} \right]. \end{aligned} \quad (9)$$

Here, $Z_{\alpha\beta} = \partial_\alpha Z_\beta - \partial_\beta Z_\alpha$, and $\tilde{Z}_{\mu\nu} = \frac{1}{2}\varepsilon_{\mu\nu\rho\sigma}Z^{\rho\sigma}$ (with $\varepsilon_{0123} = +1$) are the field strength tensor. Similarly $F_{\mu\nu}$ is the electromagnetic field tensor. However, f_4^V, h_1^V, h_2^V are three CP -violating, and f_5^V, h_3^V, h_4^V are three CP -conserving couplings ($V = \gamma, Z$). All couplings are zero at the tree-level in the SM. In the Lagrangian, the h_2^V and h_4^V couplings are dim-8, while the other four are dim-6.

The couplings in Eq. 9 are related to the coefficients given in Eqs. (2-5) under the $SU(2)_L \times U(1)_Y$ gauge invariance [67]. The anomalous couplings for the ZZV interaction, involving two on-shell Z -bosons and one off-shell $V = \gamma$ or Z boson with CP -conserving, are given below [65]:

$$f_5^Z = 0, \quad (10)$$

$$f_5^\gamma = \frac{v^2 m_Z^2}{4 c_\omega s_\omega} \frac{C_{\tilde{B}W}}{\Lambda^4}. \quad (11)$$

However, the CP -violating couplings are the follows

$$f_4^Z = \frac{m_Z^2 v^2 \left(c_\omega^2 \frac{C_{WW}}{\Lambda^4} + 2 c_\omega s_\omega \frac{C_{BW}}{\Lambda^4} + 4 s_\omega^2 \frac{C_{BB}}{\Lambda^4} \right)}{2 c_\omega s_\omega}, \quad (12)$$

$$f_4^\gamma = - \frac{m_Z^2 v^2 \left(-c_\omega s_\omega \frac{C_{WW}}{\Lambda^4} + \frac{C_{BW}}{\Lambda^4} (c_\omega^2 - s_\omega^2) + 4 c_\omega s_\omega \frac{C_{BB}}{\Lambda^4} \right)}{4 c_\omega s_\omega}. \quad (13)$$

In the equations below, s_ω and c_ω represent the sine and cosine of the weak mixing angles θ_w . The CP -conserving coupling, featuring one on-shell Z -boson and a photon with one extra off-shell $V = Z$ or γ boson, are given as follows [65].

$$h_3^Z = \frac{v^2 m_Z^2}{4 c_\omega s_\omega} \frac{C_{\tilde{B}W}}{\Lambda^4}, \quad (14)$$

$$h_4^Z = h_4^\gamma = h_3^\gamma = 0. \quad (15)$$

Furthermore, the CP -violating couplings are characterized by the following expressions.

$$h_1^Z = \frac{m_Z^2 v^2 \left(-c_\omega s_\omega \frac{C_{WW}}{\Lambda^4} + \frac{C_{BW}}{\Lambda^4} (c_\omega^2 - s_\omega^2) + 4 c_\omega s_\omega \frac{C_{BB}}{\Lambda^4} \right)}{4 c_\omega s_\omega}, \quad (16)$$

$$h_2^Z = h_2^\gamma = 0, \quad (17)$$

$$h_1^\gamma = - \frac{m_Z^2 v^2 \left(s_\omega^2 \frac{C_{WW}}{\Lambda^4} - 2 c_\omega s_\omega \frac{C_{BW}}{\Lambda^4} + 4 c_\omega^2 \frac{C_{BB}}{\Lambda^4} \right)}{4 c_\omega s_\omega}. \quad (18)$$

The connections of C_{WW}/Λ^4 , C_{BW}/Λ^4 , C_{BB}/Λ^4 , and $C_{\tilde{B}W}/\Lambda^4$ in Equations (11)-(14), (16), (18) define the dim-8 aNTGC that CP -conserving $C_{\tilde{B}W}/\Lambda^4$ and CP -violating C_{WW}/Λ^4 , C_{BB}/Λ^4 , C_{BW}/Λ^4 couplings. The experimental results on these dim-8 couplings are determined through the $pp \rightarrow Z\gamma \rightarrow \nu\bar{\nu}\gamma$ process, including neutrino decay, at LHC with a

luminosity of 36.1 fb^{-1} at $\sqrt{s} = 13 \text{ TeV}$ [68]. The experimental limits in this study, at a 95% Confidence Level (C.L.), are provided as follows:

$$-1.1 \text{ TeV}^{-4} < \frac{C_{\tilde{B}W}}{\Lambda^4} < 1.1 \text{ TeV}^{-4}, \quad (19)$$

$$-2.3 \text{ TeV}^{-4} < \frac{C_{WW}}{\Lambda^4} < 2.3 \text{ TeV}^{-4}, \quad (20)$$

$$-0.65 \text{ TeV}^{-4} < \frac{C_{BW}}{\Lambda^4} < 0.64 \text{ TeV}^{-4}, \quad (21)$$

$$-0.24 \text{ TeV}^{-4} < \frac{C_{BB}}{\Lambda^4} < 0.24 \text{ TeV}^{-4}. \quad (22)$$

II. EVENT GENERATION AND CUT-BASED ANALYSIS

The investigation of the $C_{\tilde{B}W}/\Lambda^4$, C_{BW}/Λ^4 , C_{BB}/Λ^4 , and C_{WW}/Λ^4 couplings, which affect the $ZZ\gamma$ and $Z\gamma\gamma$ couplings within the $\mu^-\gamma \rightarrow Zl^- \rightarrow l^-\tilde{\nu}_l\nu_l$ process at the FCC and SPPC, operating at $\sqrt{s} = 24.5$ and 20.2 TeV with integrated luminosities of $\mathcal{L}_{int} = 5\text{fb}^{-1}$ and 42.8 fb^{-1} , respectively. Signal-background analyses for the $\mu^-\gamma \rightarrow Zl^- \rightarrow l^-\tilde{\nu}_l\nu_l$ process are produced, incorporating the aNTGCs via the Universal FeynRules Output(UFO) into MadGraph5aMC@NLO [69]. The study focuses on the $\nu\nu\ell$ final state, presuming the Z -boson decays into a neutrino pair during $Z\ell$ production, where ℓ denotes charged leptons ($\ell = e, \mu$). Processes involving Z -boson decay into neutrinos offer distinct advantages over those involving decay into charged leptons ($\ell^-\ell^+$) or hadrons ($q\bar{q}$). Hadronic decay leads to challenges in obtaining clean data due to significant QCD backgrounds. In contrast, neutrino pair decay provides a higher branching ratio for the Z -boson, offering enhanced sensitivity in higher-energy regions.

This study based the EPA, also known as the Weizsacker Williams Approximation (WWA) [70, 71], as the primary theoretical framework for evaluating sensitivity of the $\mu^-\gamma \rightarrow Zl^- \rightarrow l^-\tilde{\nu}_l\nu_l$ process. The analysis aims to evaluate the potential of FCC and SPPC muon-proton colliders in probing anomalous $Z\gamma\gamma$ and $ZZ\gamma$ triple vertices. Within this framework, the incoming photon from the proton beam is considered using the WWA. The subsequent equation illustrates the photon distribution emitted by a proton beam [72, 73].

$$f_{\gamma^*(x)} = \frac{\alpha}{\pi E_p} \left\{ [1-x] \left[\varphi\left(\frac{Q_{max}^2}{Q_0^2}\right) - \varphi\left(\frac{Q_{min}^2}{Q_0^2}\right) \right], \right. \quad (23)$$

where the function φ is given as:

$$\begin{aligned} \varphi(\theta) = & (1+ky) \left[-In\left(1+\frac{1}{\theta}\right) + \sum_{s=1}^3 \frac{1}{s(1+\theta)^s} \right] + \frac{y(1-l)}{4\theta(1+\theta)^3} \\ & + m\left(1+\frac{y}{4}\right) \left[In\left(\frac{1-l+\theta}{1+\theta}\right) + \sum_{s=1}^3 \frac{b^s}{s(1+\theta)^s} \right]. \end{aligned} \quad (24)$$

Here,

$$y = \frac{x^2}{(1-x)}, \quad (25)$$

$$k = \frac{1+\mu_p^2}{4} + \frac{4m_p^2}{Q_0^2} \approx 7.16, \quad (26)$$

$$l = 1 - \frac{4m_p^2}{Q_0^2} \approx -3.96, \quad (27)$$

$$m = \frac{\mu_p^2 - 1}{b^4} \approx 0.028. \quad (28)$$

The cross-section of the total process $\mu^- \gamma \rightarrow Z l^- \rightarrow l^- \tilde{\nu}_l \nu_l$ is thus obtained from:

$$\sigma = \int f_\gamma(x) d\hat{\sigma} dE_1. \quad (29)$$

The Feynman diagrams for the $\mu^- \gamma \rightarrow Z l^- \rightarrow l^- \tilde{\nu}_l \nu_l$ process are given in Figure 1. Here, the two diagrams on the bottom include contributions from the Standard Model, while the two Feynman diagrams on the top include the contributions coming beyond the Standard Model, associated with anomalous $Z\gamma\gamma$ and $ZZ\gamma$ vertices. In the study, kinematic cuts

need to be applied to separate the signal from the relevant background, and after selecting appropriate cuts, the relevant background is suppressed. We obtained the optimized cuts with the help of the kinematic distributions of the variables given in Fig. 2-4. Beholding the separation point of the signals and backgrounds in the related figures and the number of events, we obtained the transverse momentum and the pseudo-rapidity of the charged lepton $p_T^l > 80$, $\eta_l < 2$ and the transverse missing energy $\cancel{E}_T > 300$, based on the final state particles of the process $\mu^- \gamma \rightarrow Z l^- \rightarrow l^- \tilde{\nu}_l \nu_l$. The number of events after the applied cuts is given step-by-step in Table-I for the signals and the related backgrounds at FCC- μp and SPPC- μp . Here, all couplings are chosen 1 TeV^{-4} . After the applied cuts, the SM and the $W^- \nu_l \rightarrow l^- \tilde{\nu}_l \nu_l$ background events decreased dramatically compering with the preselection case. Truncated background events allow more confident analysis to get the sensitivities on the dim-8 aNTGCs. On the other hand, we give the total cross-sections of the process $\mu^- \gamma \rightarrow Z l^- \rightarrow l^- \tilde{\nu}_l \nu_l$ in terms of the anomalous C_{BB}/Λ^4 , C_{BW}/Λ^4 , C_{WW}/Λ^4 , and $C_{\tilde{B}W}/\Lambda^4$ couplings at FCC and SPPC in Fig. 5-6. In these figures, each coupling is set individually. Here, only one of the aNTGC couplings is non-zero at any time, while the others are zero. These figures show the deviation of the couplings from the SM. In these figures, C_{BB}/Λ^4 is more significant than the other couplings at both FCC and SPPC.

III. EXPECTED SENSITIVITIES ON DIM-8 ANTGC

To investigate the sensitivities of the anomalous C_{BB}/Λ^4 , C_{BW}/Λ^4 , C_{WW}/Λ^4 , and $C_{\tilde{B}W}/\Lambda^4$ couplings at %95 C.L., a χ^2 test with systematic errors was applied. The χ^2 test is defined as follows:

$$\chi^2(f_{T,j}/\Lambda^4) = \left(\frac{\sigma_{SM}(\sqrt{s}) - \sigma_{Total}(\sqrt{s}, f_{T,j}/\Lambda^4)}{\sigma_{SM}(\sqrt{s}) \sqrt{(\delta_{sys})^2 + (\delta_{st})^2}} \right)^2, \quad (30)$$

Here, $\sigma_{SM}(\sqrt{s})$ represents the cross-section of the SM background, and $\sigma_{total}(\sqrt{s}, f_{T,j}/\Lambda^4)$ is the total cross-section of both the new physics coming from beyond the SM and the SM background. $\delta_{st} = \frac{1}{\sqrt{N_{SM}}}$ and δ_{sys} are the statistical error and systematic uncertainty, respectively. The event number of the SM background is defined as $N_{SM} = \mathcal{L} \times \sigma_{SM}$, where \mathcal{L} is the integrated luminosity. Systematic uncertainties from various sources have been included in the χ^2 analysis [74]. In the study, systematic uncertainties of 0%, 3%, and

TABLE I: Events for the process $\mu^-\gamma \rightarrow Zl^- \rightarrow l^-\tilde{\nu}_l\nu_l$ for various couplings and SM background.

Background						Signals						
Cuts	Standard Model		$W^-\nu_l \rightarrow l^-\tilde{\nu}_l\nu_l$		C_{BB}/Λ^4		$C_{\tilde{B}W}/\Lambda^4$		C_{BW}/Λ^4		C_{WW}/Λ^4	
FCC- μp	Events	$\epsilon[\%]$	Events	$\epsilon[\%]$	Events	$\epsilon[\%]$	Events	$\epsilon[\%]$	Events	$\epsilon[\%]$	Events	$\epsilon[\%]$
Presel.	293	—	7200	—	4131	—	830	—	613	—	312	—
$p_T^l > 80$ GeV	47	16.0	1451	20.2	3883	94.0	584	70.3	368	60.0	65	20.9
$\cancel{E}_T > 300$ GeV	6	12.8	64	4.4	3841	99.0	542	92.8	328	88.9	23	36.1
$\eta^l < 2.0$	5	75.6	63	98.6	3838	99.9	540	99.7	326	99.4	22	94.9
SPPC- μp												
Presel.	3360	—	55982	—	17483	—	4682	—	3968	—	3429	—
$p_T^l > 100$ GeV	439	13.1	7168	12.8	14546	83.1	2109	34.0	1196	30.1	508	14.8
$\cancel{E}_T > 400$ GeV	24	5.5	205	2.9	14108	96.9	1727	81.8	805	67.2	96	18.8
$\eta^l < 2.0$	24	100.0	205	100.0	14108	100.0	1727	100.0	805	100.0	96	100.0

5% have been considered. Obtained sensitivities on aNTGs via the process $\mu^-\gamma \rightarrow Zl^- \rightarrow l^-\tilde{\nu}_l\nu_l$ at FCC- μp and SPPC- μp under various systematic uncertainties are given in Table II.

IV. CONCLUSIONS

This study introduces a phenomenological approach using cut-based techniques to explore the constraints on the CP-conserving $C_{\tilde{B}W}/\Lambda^4$ coupling and CP-violating C_{BW}/Λ^4 , C_{WW}/Λ^4 and C_{BB}/Λ^4 couplings via the process $\mu^-\gamma \rightarrow Zl^- \rightarrow l^-\tilde{\nu}_l\nu_l$ at the FCC and SPPC. It emphasizes the importance of p_T^l , η and the transverse missing energy \cancel{E}_T in distinguishing signals from relevant background. By using the cut-based analysis, we determine the sensitivities of each anomalous coupling using the χ^2 method for the FCC- μp and SPPC- μp colliders operating at $\sqrt{s} = 24.5$ and 20.2 TeV with $\mathcal{L}_{int} = 5$ and 42.8 fb^{-1} , respectively. Comparisons are made with the experimental research on $\nu\nu\gamma$ production at the LHC running at $\sqrt{s} = 13$ TeV, as well as theoretical studies concerning $\nu\nu\gamma$ production at the HL-LHC and HE-LHC, and $Z\gamma \rightarrow \nu\nu\gamma$ production at the muon collider [23, 75].

TABLE II: Sensitivities at 95% C.L. on the anomalous $Z\gamma\gamma$ and $ZZ\gamma$ couplings via the process $\mu^-\gamma \rightarrow Zl^- \rightarrow l^-\tilde{\nu}_l\nu_l$ under the systematic uncertainties of $\delta_{sys} = 0\%, 3\%$, and 5% are represented.

			FCC- μp	SPPC- μp
Couplings	LHC Bound	Systematic Errors	Our Projection	Our Projection
C_{BB}/Λ^4	[−0.24; 0.24]	$\delta = 0\%$	[−0.06845; 0.070019]	[−0.06606; 0.05050]
		$\delta = 3\%$	[−0.06852; 0.07009]	[−0.06638; 0.05082]
		$\delta = 5\%$	[−0.06865; 0.07022]	[−0.06695; 0.05138]
C_{BW}/Λ^4	[−0.65; 0.64]	$\delta = 0\%$	[−0.23623; 0.23815]	[−0.20663; 0.19155]
		$\delta = 3\%$	[−0.23649; 0.23840]	[−0.20776; 0.19269]
		$\delta = 5\%$	[−0.23693; 0.23885]	[−0.20973; 0.19466]
$C_{\tilde{B}W}/\Lambda^4$	[−1.10; 1.10]	$\delta = 0\%$	[−0.18662; 0.18422]	[−0.15791; 0.15126]
		$\delta = 3\%$	[−0.18682; 0.18442]	[−0.15879; 0.15214]
		$\delta = 5\%$	[−0.18716; 0.18477]	[−0.16032; 0.15368]
C_{WW}/Λ^4	[−2.30; 2.30]	$\delta = 0\%$	[−0.61912; 0.62072]	[−0.51383; 0.52211]
		$\delta = 3\%$	[−0.61978; 0.62138]	[−0.51679; 0.52506]
		$\delta = 5\%$	[−0.62094; 0.62254]	[−0.52193; 0.53020]

While our results outperform those of the HL-LHC and the HE-LHC in general, they are 2-3 times worse than the sensitivities achieved by the muon collider. Consequently, our findings suggest that the μp collisions at FCC and SPPC with $\sqrt{s}=24.5$ and 20.2 TeV could enhance the sensitivity limits on C_{BB}/Λ^4 , $C_{\tilde{B}W}/\Lambda^4$, C_{BW}/Λ^4 , C_{WW}/Λ^4 parameters defining the aNTGC $ZZ\gamma$ and $Z\gamma\gamma$ compared to the latest experimental results of LHC and the phenomenological results of future hadron-hadron colliders.

Acknowledgements

The numerical calculations reported in this paper were fully performed at TUBITAK ULAKBIM, High Performance and Grid Computing Center (TRUBA resources).

V. DATA AVAILABILITY STATEMENT

This manuscript has no associated data or the data will not be deposited. [Authors' comment: Data will be made available upon reasonable request.]

- [1] U. Baur and D. Rainwater, Phys. Rev. D **62**, 113011 (2000) [arXiv:hep-ph/0008063].
- [2] S. Spor and M. Köksal, Phys. Lett. B **820** (2021), 136533 doi:10.1016/j.physletb.2021.136533 [arXiv:2009.05848 [hep-ph]].
- [3] A. A. Billur, M. Köksal, A. Gutiérrez-Rodríguez and M. A. Hernández-Ruiz, Eur. Phys. J. Plus **136** (2021) no.6, 697 doi:10.1140/epjp/s13360-021-01684-6 [arXiv:1909.10299 [hep-ph]].
- [4] V. Arı, A. A. Billur, S. C. İnan and M. Köksal, Nucl. Phys. B **906** (2016), 211-230 doi:10.1016/j.nuclphysb.2016.02.029 [arXiv:1506.08998 [hep-ph]].
- [5] D. Choudhury and S. D. Rindani, Phys. Lett. B **335**, 198-204 (1994) [arXiv:hep-ph/9405242].
- [6] S. Ataḡ and İ. Şahin, Phys. Rev. D **70**, 053014 (2004) [arXiv:hep-ph/0408163].
- [7] I. Ots, H. Uibo, H. Liivat, R. K. Loide and R. Saar, Nucl. Phys. B **702**, 346-356 (2004).
- [8] I. Ots, H. Uibo, H. Liivat, R. K. Loide and R. Saar, Nucl. Phys. B **740**, 212-221 (2006).
- [9] A. Gutiérrez-Rodríguez, M. A. Hernández-Ruiz and M. A. Pérez, Phys. Rev. D **80**, 017301 (2009) [arXiv:0808.0945 [hep-ph]].
- [10] B. Ananthanarayan, S. K. Garg, M. Patra and S. D. Rindani, Phys. Rev. D **85**, 034006 (2012) [arXiv:1104.3645 [hep-ph]].
- [11] B. Ananthanarayan, J. Lahiri, M. Patra and S. D. Rindani, JHEP **08**, 124 (2014) [arXiv:1404.4845 [hep-ph]].
- [12] R. Rahaman and R. K. Singh, Eur. Phys. J. C **76**, 539 (2016) [arXiv:1604.06677 [hep-ph]].
- [13] R. Rahaman and R. K. Singh, Eur. Phys. J. C **77**, 521 (2017) [arXiv:1703.06437 [hep-ph]].
- [14] J. Ellis, S. F. Ge, H. J. He and R. Q. Xiao, Chin. Phys. C **44**, 063106 (2020) [arXiv:1902.06631 [hep-ph]].
- [15] Q. Fu, J. C. Yang, C. X. Yue and Y. C. Guo, Nucl. Phys. B **972**, 115543 (2021) [arXiv:2102.03623 [hep-ph]].
- [16] J. Ellis, H. J. He and R. Q. Xiao, Sci. China Phys. Mech. Astron. **64**, 221062 (2021) [arXiv:2008.04298 [hep-ph]].

- [17] J. C. Yang, Y. C. Guo and L. H. Cai, Nucl. Phys. B **977**, 115735 (2022) [arXiv:2111.10543 [hep-ph]].
- [18] S. Spor, E. Gurkanli and M. Köksal, Nucl. Phys. B **979**, 115785 (2022) [arXiv:2203.02352 [hep-ph]].
- [19] U. Baur and E. L. Berger, Phys. Rev. D **47**, 4889 (1993).
- [20] A. Senol, H. Denizli, A. Yilmaz, I. T. Cakir, K. Y. Oyulmaz, O. Karadeniz and O. Cakir, Nucl. Phys. B **935**, 365-376 (2018) [arXiv:1805.03475 [hep-ph]].
- [21] R. Rahaman and R. K. Singh, Nucl. Phys. B **948**, 114754 (2019) [arXiv:1810.11657 [hep-ph]].
- [22] A. Senol, H. Denizli, A. Yilmaz, I. T. Cakir and O. Cakir, Acta Phys. Pol. B **50**, 1597 (2019) [arXiv:1906.04589 [hep-ph]].
- [23] A. Senol, H. Denizli, A. Yilmaz, I. T. Cakir and O. Cakir, Phys. Lett. B **802**, 135255 (2020) [arXiv:1910.03843 [hep-ph]].
- [24] A. Yilmaz, A. Senol, H. Denizli, I. T. Cakir and O. Cakir, Eur. Phys. J. C **80**, 173 (2020) [arXiv:1906.03911 [hep-ph]].
- [25] A. Yilmaz, Nucl. Phys. B **969**, 115471 (2021) [arXiv:2102.01989 [hep-ph]].
- [26] A. I. Hernández-Juárez, A. Moyotl and G. Tavares-Velasco, Eur. Phys. J. C **81**, 304 (2021) [arXiv:2102.02197 [hep-ph]].
- [27] A. Biekötter, P. Gregg, F. Krauss and M. Schönherr, Phys. Lett. B **817**, 136311 (2021) [arXiv:2102.01115 [hep-ph]].
- [28] D. Lombardi, M. Wiesemann, G. Zanderighi, Phys. Lett. B **824**, 136846 (2022).
- [29] A. I. Hernández-Juárez and G. Tavares-Velasco, [arXiv:2203.16819 [hep-ph]].
- [30] C. Geng *et al.* [ATLAS Collaboration], PoS **DIS2019**, 286 (2019).
- [31] G. J. Gounaris, J. Layssac and F. M. Renard, Phys. Rev. D **67**, 013012 (2003) [arXiv:hep-ph/0211327].
- [32] A. Belloni, A. Freitas, J. Tian, J. Alcaraz Maestre, A. Apyan, B. Azartash-Namin, P. Azzurri, S. Banerjee, J. Beyer and S. Bhattacharya, *et al.* [arXiv:2209.08078 [hep-ph]].
- [33] J. P. Delahaye, M. Diemoz, K. Long, B. Mansoulié, N. Pastrone, L. Rivkin, D. Schulte, A. Skrinsky and A. Wulzer, “Muon Colliders,” (2019) [arXiv:1901.06150 [physics.acc-ph]].
- [34] K. R. Long, D. Lucchesi, M. A. Palmer, N. Pastrone, D. Schulte and V. Shiltsev, Nat. Phys. **17**, 289-292 (2021).
- [35] The CEPC Study Group, [arXiv:1811.10545 [hep-ex]].

- [36] R. B. Palmer, Rev. Accel. Sci. Tech. **7**, 137-159 (2014).
- [37] M. Antonelli, M. Boscolo, R. D. Nardo and P. Raimondi, Nucl. Instrum. Meth. A **807**, 101-107 (2016) [arXiv:1509.04454 [physics.acc-ph]].
- [38] M-H. Wang, Y. Nosochkov, Y. Cai and M. Palmer, JINST **11**, P09003 (2016).
- [39] D. Neuffer and V. Shiltsev, JINST **13**, T10003 (2018) [arXiv:1811.10694 [physics.acc-ph]].
- [40] M. Boscolo, J-P. Delahaye and M. Palmer, Rev. Accel. Sci. Tech. **10**, 189-214 (2019) [arXiv:1808.01858 [physics.acc-ph]].
- [41] B. Bogomilov *et al.* [MICE Collaboration], Nature **578**, 53-59 (2020) [arXiv:1907.08562 [physics.acc-ph]].
- [42] D. Buttazzo, D. Redigolo, F. Sala and A. Tesi, JHEP **11**, 144 (2018) [arXiv:1807.04743 [hep-ph]].
- [43] M. Köksal, A. A. Billur, A. Gutiérrez-Rodríguez and M. A. Hernández-Ruiz, Int. J. Mod. Phys. A **34**, 1950076 (2019) [arXiv:1811.01188 [hep-ph]].
- [44] A. Costantini, F. D. Lillo, F. Maltoni, L. Mantani, O. Mattelaer, R. Ruiz and X. Zhao, JHEP **09**, 80 (2020) [arXiv:2005.10289 [hep-ph]].
- [45] W. Yin and M. Yamaguchi, “Muon $g - 2$ at multi-TeV muon collider,” (2020) [arXiv:2012.03928 [hep-ph]].
- [46] M. Ruhdorfer, E. Salvioni and A. Weiler, SciPost Phys. **8**, 027 (2020) [arXiv:1910.04170 [hep-ph]].
- [47] M. Chiesa, F. Maltoni, L. Mantani, B. Mele, F. Piccinini and X. Zhao, JHEP **09**, 98 (2020) [arXiv:2003.13628 [hep-ph]].
- [48] P. Bandyopadhyay and A. Costantini, Phys. Rev. D **103**, 015025 (2021) [arXiv:2010.02597 [hep-ph]].
- [49] T. Han, S. Li, S. Su, W. Su and Y. Wu, Phys. Rev. D **104**, 055029 (2021) [arXiv:2102.08386 [hep-ph]].
- [50] W. Liu and K-P. Xie, JHEP **04**, 15 (2021) [arXiv:2101.10469 [hep-ph]].
- [51] T. Han, Z. Liu, L.-T. Wang and X. Wang, Phys. Rev. D **103**, 075004 (2021) [arXiv:2009.11287 [hep-ph]].
- [52] R. Capdevilla, F. Meloni, R. Simoniello and J. Zurita, JHEP **06**, 133 (2021) [arXiv:2102.11292 [hep-ph]].
- [53] S. Bottaro, A. Strumia and N. Vignaroli, JHEP **06**, 143 (2021) [arXiv:2103.12766 [hep-ph]].

- [54] R. Capdevilla, D. Curtin, Y. Kahn and G. Krnjaic, Phys. Rev. D **103**, 075028 (2021) [arXiv:2006.16277 [hep-ph]].
- [55] G-Y. Huang, F. S. Queiroz and W. Rodejohann, Phys. Rev. D **103**, 095005 (2021) [arXiv:2101.04956 [hep-ph]].
- [56] P. Asadi, R. Capdevilla, C. Cesarotti and S. Homiller, JHEP **10**, 182 (2021) [arXiv:2104.05720 [hep-ph]].
- [57] T. Han, D. Liu, I. Low and X. Wang, Phys. Rev. D **103**, 013002 (2021) [arXiv:2008.12204 [hep-ph]].
- [58] R. Franceschini and M. Greco, Symmetry **13**, 851 (2021) [arXiv:2104.05770 [hep-ph]].
- [59] M. Chiesa, B. Mele and F. Piccinini, “Multi Higgs production via photon fusion at future multi-TeV muon colliders,” (2021) [arXiv:2109.10109 [hep-ph]].
- [60] D. Buttazzo and P. Paradisi, Phys. Rev. D **104**, 075021 (2021) [arXiv:2012.02769 [hep-ph]].
- [61] G-Y. Huang, S. Jana, F. S. Queiroz and W. Rodejohann, Phys. Rev. D **105**, 015013 (2022) [arXiv:2103.01617 [hep-ph]].
- [62] S. Spor and M. Köksal, CJP **101**, 10 (2023) [arXiv:2201.00787 [hep-ph]].
- [63] J-C. Yang, X-Y. Han, Z-B. Qin, T. Li and Y-C. Guo, JHEP **2022**, 74 (2022) [arXiv:2204.10034 [hep-ph]].
- [64] M. Forslund and P. Meade, JHEP **2022**, 185 (2022) [arXiv:2203.09425 [hep-ph]].
- [65] C. Degrande, JHEP **02**, 101 (2014) [arXiv:1308.6323 [hep-ph]].
- [66] G. J. Gounaris, J. Layssac and F. M. Renard, Phys. Rev. D **61**, 073013 (2000) [arXiv:hep-ph/9910395].
- [67] R. Rahaman, Indian Institute of Science Education and Research, PhD thesis (2020) [arXiv:2007.07649 [hep-ph]].
- [68] M. Aaboud *et al.* [ATLAS Collaboration], JHEP **12**, 010 (2018) [arXiv:1810.04995 [hep-ex]].
- [69] J. Alwall, R. Frederix, S. Frixione, V. Hirschi, F. Maltoni, O. Mattelaer, H. S. Shao, T. Stelzer, P. Torrielli and M. Zaro, JHEP **07**, 079 (2014) [arXiv:1405.0301 [hep-ph]].
- [70] C. F. von Weizsäcker, *Z. Phys.* **88**, 612 (1934).
- [71] E. J. Williams, *Kong. Dan. Vid. Sel. Mat. Fys. Medd.* **13N4**, 1 (1935).
- [72] V. M. Budnev, I. F. Ginzburg, G. V. Meledin and V. G. Serbo, *Phys. Rep.* **15**, 181 (1975).
- [73] M. S. Chen, T. P. Cheng, I. J. Muzinich and H. Terazawa, *Phys. Rev. D* **7**, 3485 (1973).
- [74] G. Khoriauli, *Nuovo Cimento B* **123**, 1327-1330 (2008).

- [75] A. Senol, S. Spor, E. Gurkanli, V. Cetinkaya, H. Denizli and M. Koksal, Eur. Phys. J. P **137**, 1354 (2022).

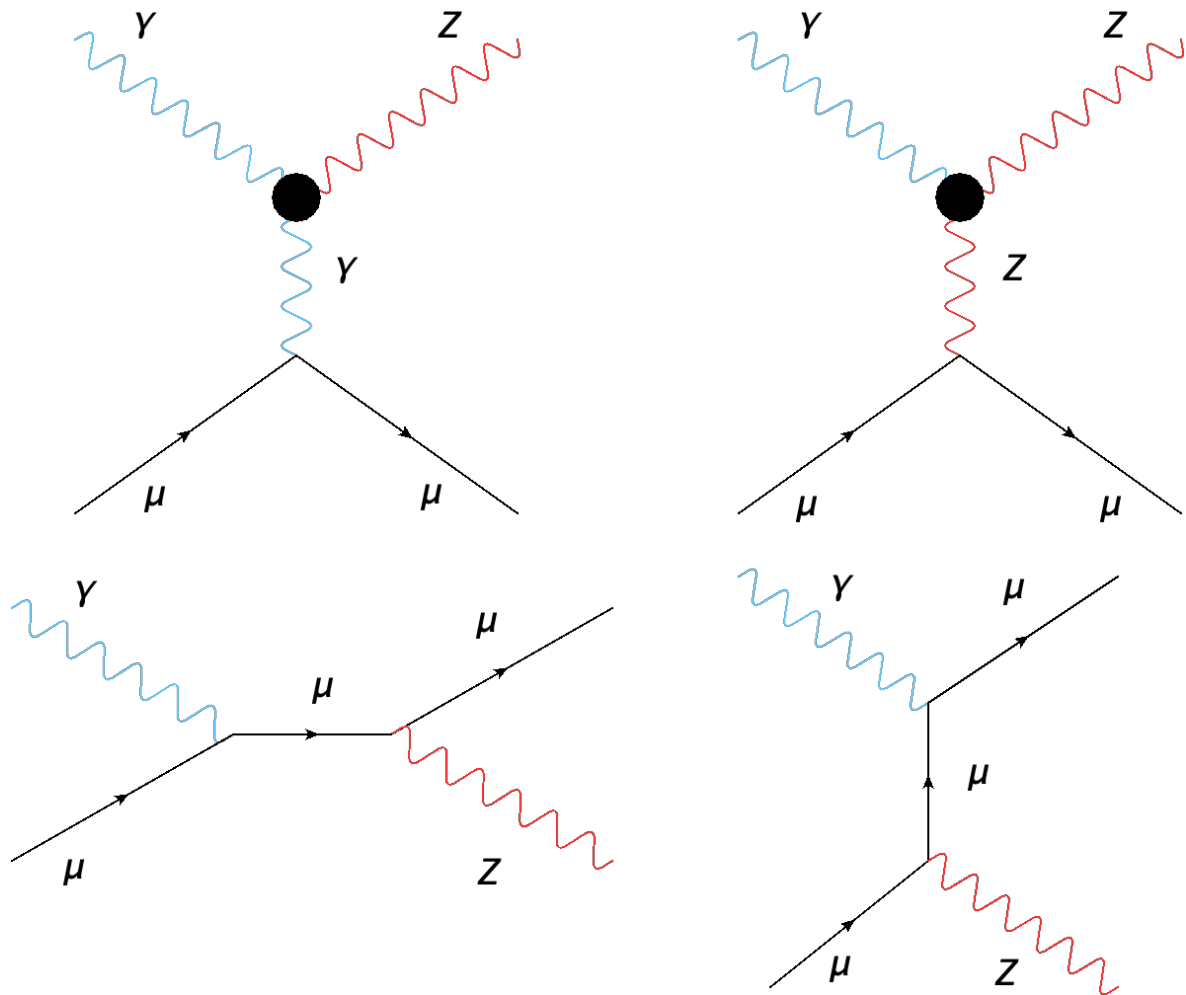


FIG. 1: Diagrams for the process $\mu^- \gamma \rightarrow Z l^-$ including the anomalous $ZZ\gamma$ and $Z\gamma\gamma$ couplings. New physics contributions are shown by a black circle. Rest of them are contain the Standard Model contributions.

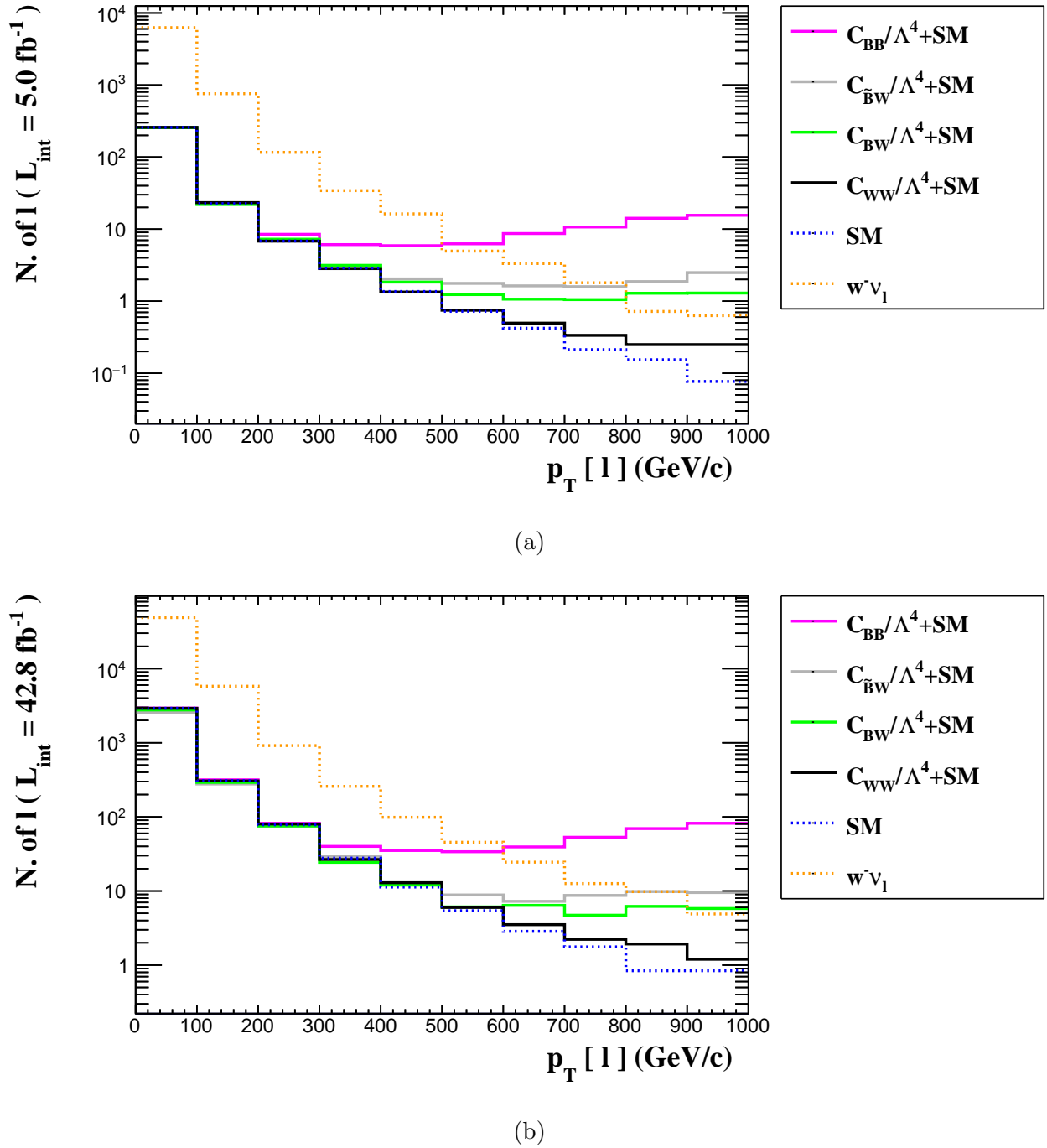


FIG. 2: (a) The number of events as a function of the p_T^ℓ for the process $\mu^- \gamma \rightarrow Zl^- \rightarrow l^- \bar{\nu}_l \nu_l$ and related backgrounds at FCC with the $\sqrt{s} = 24.5 \text{ TeV}$. (b) Same as for (a) but for SPPC with the $\sqrt{s} = 20.2 \text{ TeV}$.

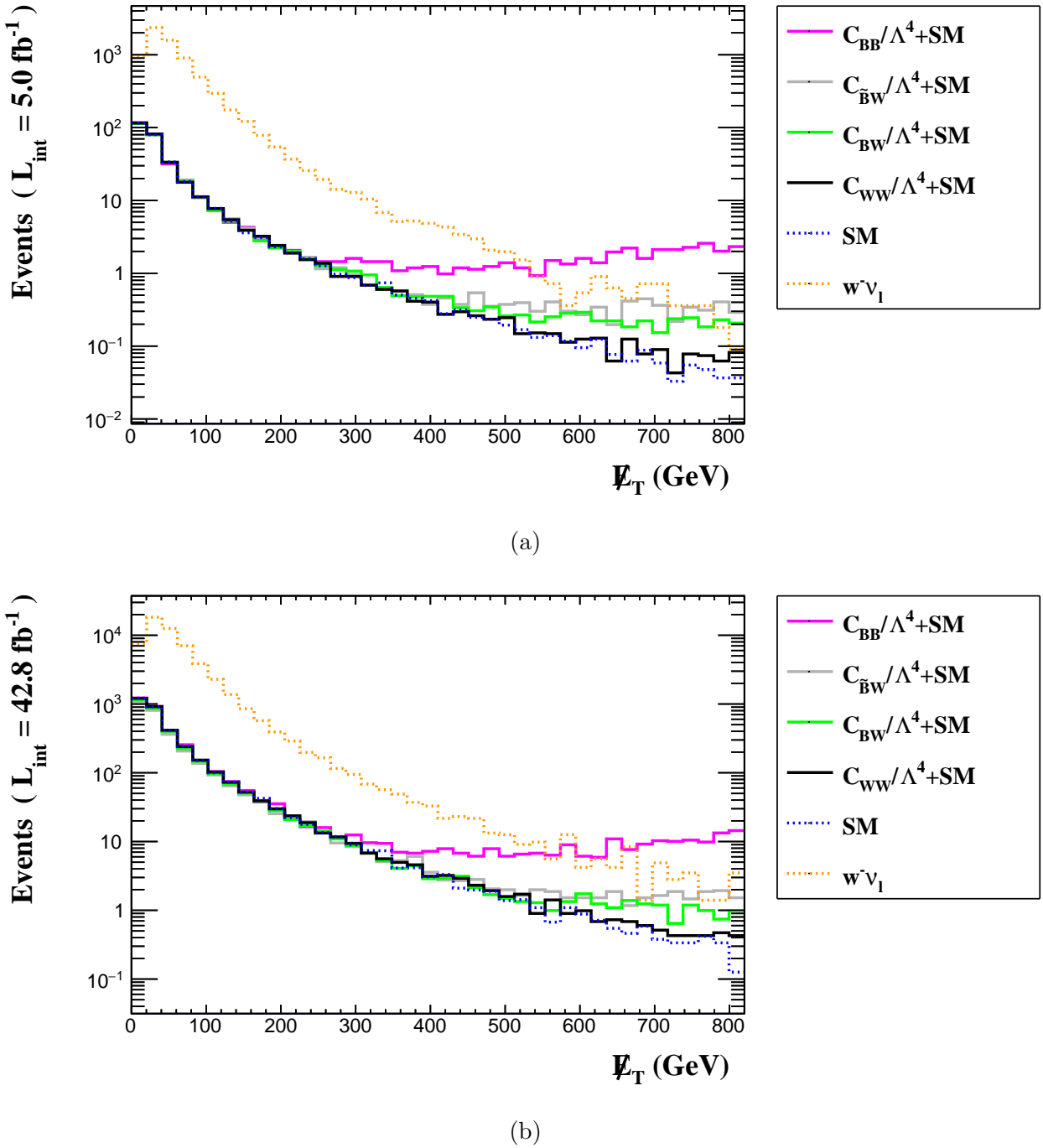


FIG. 3: (a) The number of events as a function of the \not{E}_T for the process $\mu^- \gamma \rightarrow Z l^- \rightarrow l^- \bar{\nu}_l \nu_l$ and related backgrounds at FCC with the $\sqrt{s} = 24.5 \text{ TeV}$. (b) Same as for (a) but for SPPC with the $\sqrt{s} = 20.2 \text{ TeV}$.

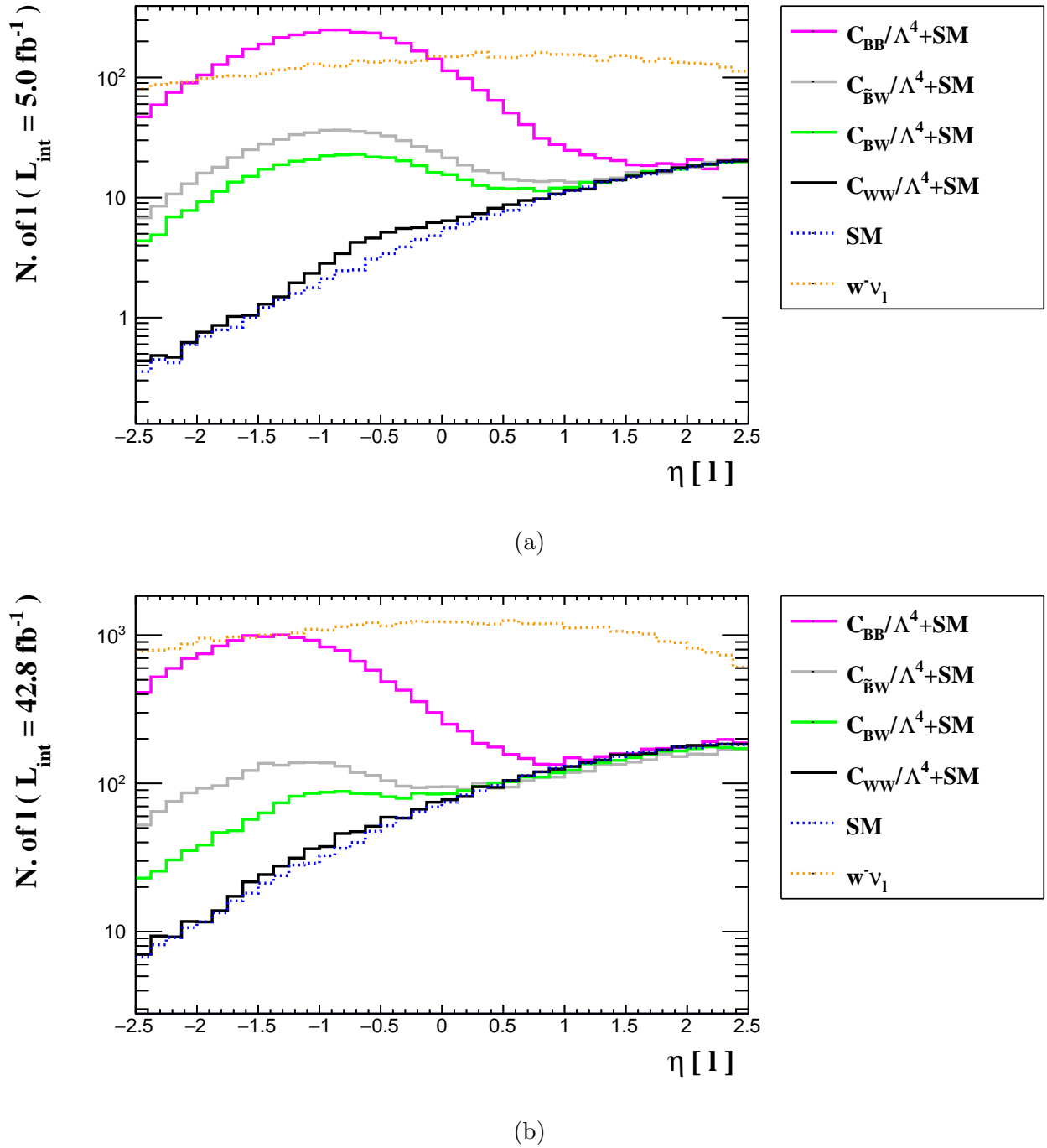


FIG. 4: (a) The number of events as a function of η_ℓ for the process $\mu^-\gamma \rightarrow Zl^- \rightarrow l^-\tilde{\nu}_l\nu_l$ and related backgrounds at FCC with the $\sqrt{s} = 24.5$ TeV. (b) Same as for (a) but for SPPC with the $\sqrt{s} = 20.2$ TeV.

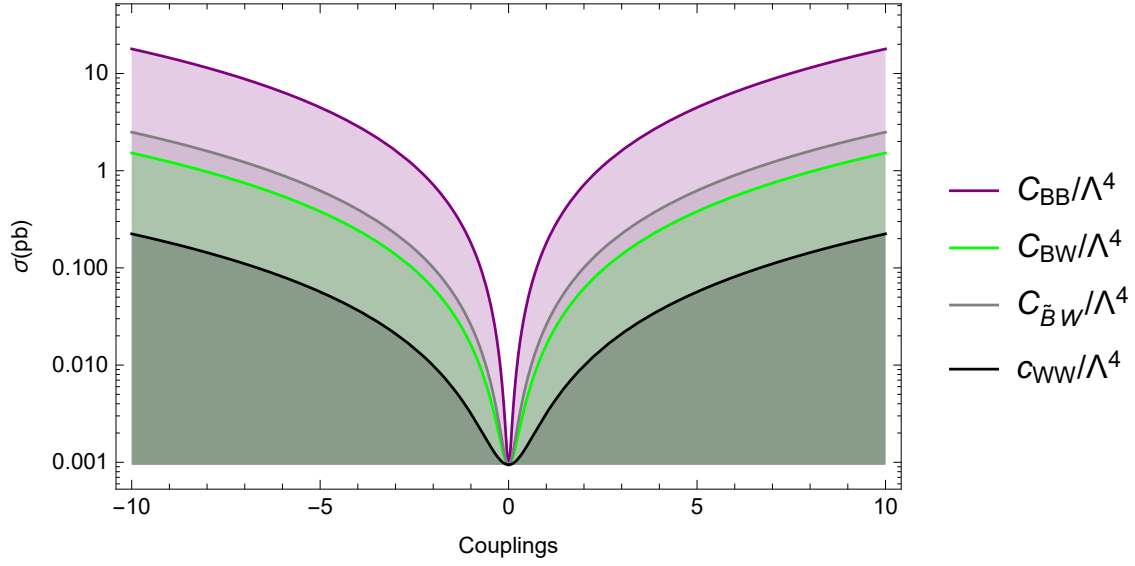


FIG. 5: Cross-sections of the process $\mu^- \gamma \rightarrow Z l^- \rightarrow l^- \tilde{\nu}_l \nu_l$ in terms of the parameters $C_{WW}/\Lambda^4, C_{BB}/\Lambda^4, C_{\tilde{B}W}/\Lambda^4, C_{BW}/\Lambda^4$ at SPPC.

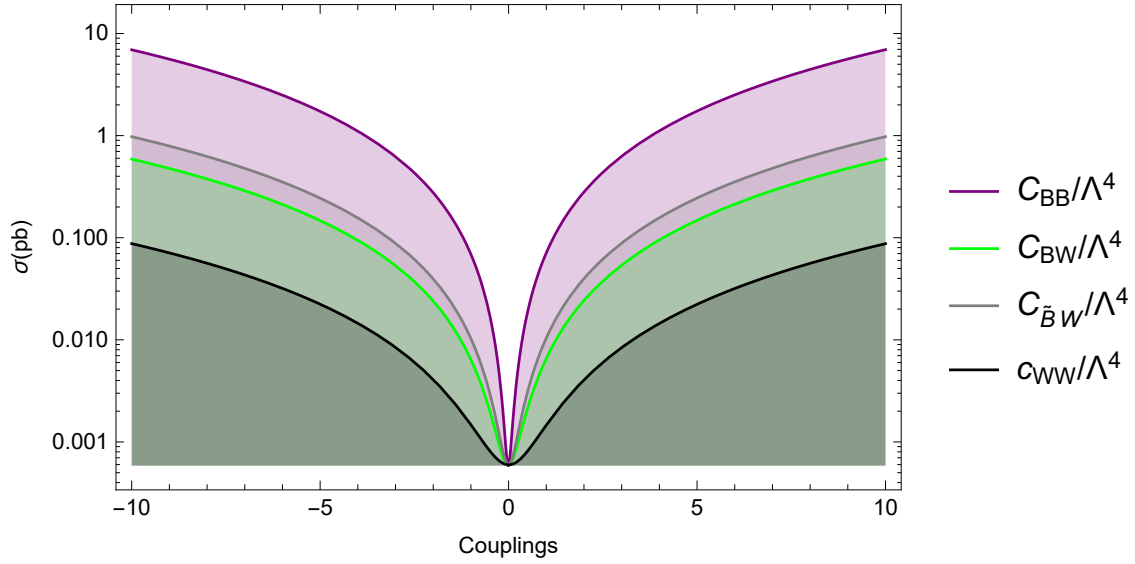


FIG. 6: Cross-sections of the process $\mu^- \gamma \rightarrow Z l^- \rightarrow l^- \tilde{\nu}_l \nu_l$ in terms of the parameters $C_{WW}/\Lambda^4, C_{BB}/\Lambda^4, C_{\tilde{B}W}/\Lambda^4, C_{BW}/\Lambda^4$ at FCC.

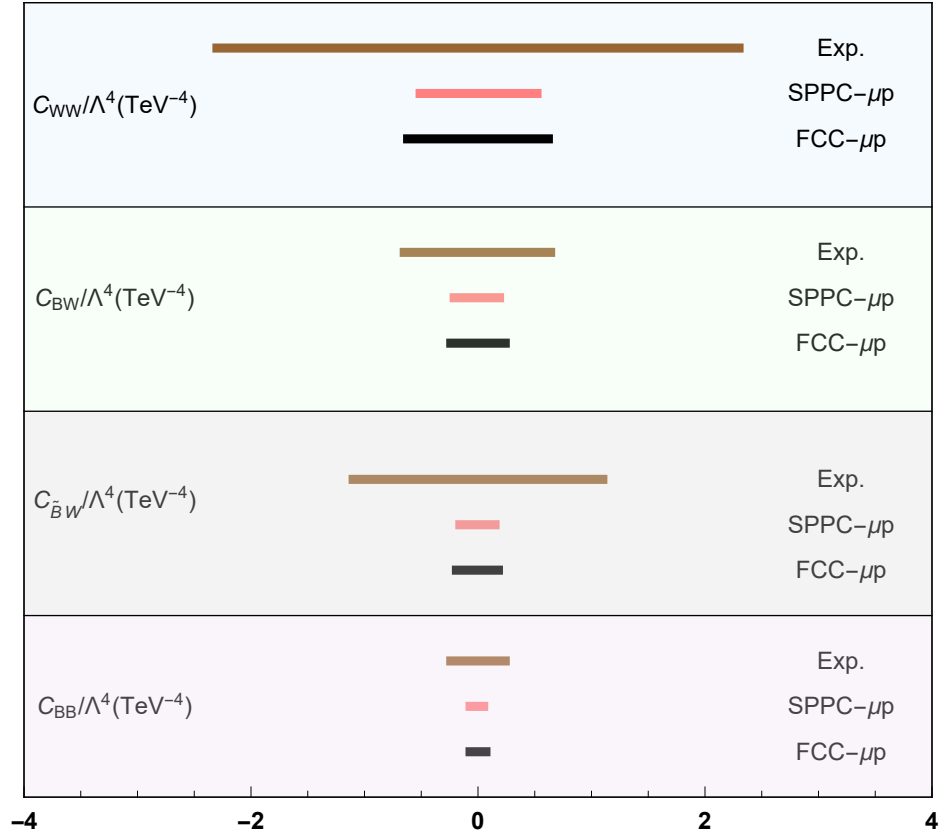


FIG. 7: Comparison of LHC bounds and obtained sensitivities on the anomalous C_{WW}/Λ^4 , C_{BB}/Λ^4 , $C_{\tilde{B}W}/\Lambda^4$, C_{BW}/Λ^4 parameters via the process $\mu^- \gamma \rightarrow Z l^- \rightarrow l^- \bar{\nu}_l \nu_l$ at FCC and SPPC.